

Enhanced COVID-19 Detection Through Combined Image Enhancement and Deep Learning Techniques

Abderrazak Benchabane*, Fella Charif

Department of electronics and telecommunications, University of Kasdi Merbah, Ouargla, Algeria

E-mail : benchabane.abderrazak@univ-ouargla.dz, cherif.fella@univ-ouargla.dz

*Corresponding author

Keywords: COVID-19, image enhancement, chest x-ray images, deep learning

Received: March 6, 2024

The rapid spread of COVID-19 has highlighted the need for automated patient data analysis to enable faster and more accurate diagnosis. Using pre-trained deep learning models on X-ray images has shown potential for effective COVID-19 detection. However, the performance of these models is highly dependent on the quality and quantity of training data. To address these challenges, enhancing the visual quality of X-ray images is critical for reliable virus detection. This study evaluates and combines three image enhancement techniques—Histogram Equalization, Contrast-Limited Adaptive Histogram Equalization (CLAHE), and Gamma Correction—to determine the optimal approach for improving detection accuracy. A dataset comprising 125 chest X-ray images from COVID-19-positive patients and 500 images from non-COVID-19 cases was used. The images were preprocessed using the enhancement techniques, and the enhanced datasets were employed to train ResNet50 and DenseNet201 models. Simulation results demonstrate that enhanced images consistently yield higher detection accuracy than unenhanced images. Among the techniques tested, combining Histogram Equalization, CLAHE, and Gamma Correction with the DenseNet201 model achieved the highest performance, attaining a remarkable accuracy of 99.03%. This outperforms previous methods, including the DarkCovidNet model, which achieved an accuracy of 98.08% on the same dataset.

Povzetek: Avtorja sta izboljšala zaznavanje COVID-19 iz rentgenskih slik prsnega koša z uporabo tehnik izboljšave slike (Histogram Equalization, CLAHE, Gamma Correction) v kombinaciji z modeli globokega učenja (ResNet50, DenseNet201).

1 Introduction

Corona disease is currently considered one of the most widespread, dangerous and fastest diseases, so it is necessary to find ways and methods to detect infected cases and diagnose them in the fastest and clearest way. RT-PCR is a nuclear-derived technique that detects the presence of genetic material specific to a pathogen, including a virus. A formal diagnosis of COVID-19 requires a laboratory test (RT-PCR) of nose and throat samples and takes at least 24 hours to produce a result. Nowadays, medical images and computerized analysis become very important tools for medical diagnosis and disease detection [1]. The radiology images show typical COVID-19 pneumonia in the lungs and the numerous complications that the virus causes in the body. The radiology imaging modalities include computed tomography (CT), radiograph X-rays, ultrasound, echocardiograms and magnetic resonance imaging (MRI). These imaging modalities optimize and greatly facilitate the process of discovering affected areas in the body [2]. Chest X-ray tests are easily available and have a low risk of radiation. On the other hand, CT scans have a high risk of radiation, are expensive, need clinical expertise to handle and are non-portable. This makes the use of X-ray scans more convenient than CT scans. A radiograph is obtained by exposing a film to X-rays that

have passed through the human body. The result is an analog image which is often sufficient to obtain a reliable diagnosis and for low-cost screening. Various studies have indicated the failure of CXR imaging in diagnosing COVID-19 and differentiating it from other types of pneumonia [3]. The radiologist cannot use X-rays to detect pleural effusion and determine the volume involved. However, regardless of the low accuracy of X-ray diagnosis of COVID-19, it remains widely used. To overcome the limitations of COVID-19 diagnostic tests using radiological images, various studies have been conducted on the use of deep learning (DL) in the analysis of radiological images [2-11]. It has also shown that image enhancement techniques can improve significantly classification performance [12, 13].

1.1 Contribution

In this paper, we investigate the impact of using image enhancement techniques as a preprocessing step to improve the accuracy of convolutional neural network (CNN) models for COVID-19 detection. Specifically, histogram equalization, Contrast Limited Adaptive Histogram Equalization (CLAHE), and gamma correction were applied to enhance chest X-ray (CXR) images before training.

The enhanced images significantly improved the visibility of key diagnostic features, such as ground-glass opacities and consolidations, which are critical for accurate COVID-19 diagnosis. The proposed preprocessing pipeline was evaluated on a challenging COVID-19 dataset with an imbalanced number of samples for both COVID and non-COVID classes. Experimental results demonstrated that the enhanced images led to a notable improvement in the classification performance of CNN models, achieving higher accuracy, sensitivity, and specificity compared to using raw images.

The rest of the paper is organized as follows: The materials and methods section contains details about our proposed technique along with some context about the state-of-the-art models that we have used. The results and Discussion section presents the experimental results including classification accuracy, sensitivity, and F1-score obtained from the proposed work. The paper is achieved by a conclusion.

1.2 Related works

Numerous studies have applied advanced artificial intelligence (AI) techniques, particularly deep learning (DL) and machine learning (ML), to detect COVID-19 using X-ray images. Zhang et al. [14] developed an anomaly detection algorithm with efficient Net for multiclass classification, achieving an accuracy of 72.77% on 43370 samples. Deng et al. [15] employed models such as SVM, CNN, ResNet50, InceptionNetV2, Xception, and VGG16 to assess health status through X-ray imaging, obtaining an accuracy of 84% using 5857 samples. Wang et al. [16] introduced a COVID-19 X-ray

image detection model based on the multi-head self-attention mechanism and residual neural network, achieving 95.52% accuracy with 5173 samples.

Transfer learning has also played a pivotal role in COVID-19 detection. Apostolopoulos et al. [17] utilized pre-trained models like VGG19, Inception ResNet v2, and MobileNet v2, achieving 96.78% accuracy on 1427 samples for COVID-19 classification. Mahmoud et al. [18] applied the CovXNet architecture, achieving 97.4% accuracy on 610 samples. Mohit Kumar et al. [19] utilized a hybrid deep learning approach for multiclass classification, achieving 98.20% accuracy on 6000 samples.

Several studies focused on binary classification tasks with high accuracy. Guefrechi et al. [20] achieved 97.20% accuracy using deep learning methods on 5000 images. Feki et al. [21] employed a deep CNN model for binary classification, reaching an accuracy of 95.30% on 216 images. Mohan et al. [22] used a hybrid deep transfer learning CNN model achieving 92% accuracy with 9220 images. Malik et al. [23] applied deep neural networks for multiclass classification, attaining 98.45% accuracy on 10017 images. Gulmez [24] explored Xception and genetic algorithms for multiclass classification, reporting an accuracy of 92.4% on 1251 images. Lastly, Zakariya et al. proposed to combine Xception, VGG-16, and VGG-19 models. They achieved an accuracy of 97.91% using 964 images.

Table 1 provides a summary of various research studies focusing on state-of-the-art models for COVID-19 detection using AI and ML techniques.

Table 1: Summary of related works on COVID-19 detection

Source	Method/Model	Samples used	Accuracy (%)
[14]	Efficient Net	43,370	72.77
[15]	SVM, CNN, ResNet50, Xception, VGG16	5,857	84.00
[16]	MHSA-ResNet neural network model	5173	95.52
[17]	VGG19, Inception ResNet v2, and MobileNet v2	1,427	96.78
[18]	CovXNet	610	97.40
[19]	Hybrid deep learning approach	6,000	98.20
[20]	Deep Learning (Resnet50)	5,000	97.20
[21]	Deep CNN (Centralized-ResNet50)	216	95.30
[22]	Deep Transfer Learning	9220	92.00
[23]	Deep Neural Networks	10,017	98.45
[24]	Xception and Genetic Algorithm	1,251	92.40
[25]	Xception+vgg-16+vgg-19	964	97.91

2 Materials and methods

2.1 Dataset generation

The Dataset of chest X-ray images used in this paper for classifying negative and positive COVID-19 cases is available at (<https://github.com/muhammedtalo/COVID-19>). It contains 125 chest x-ray images of patients

infected with the virus and 500 chest x-ray images of non-COVID-19. The data is divided into 2 classes, 50% of images were used for training and 50% for testing. Figure 1 shows some samples that have been used in our simulation [6].

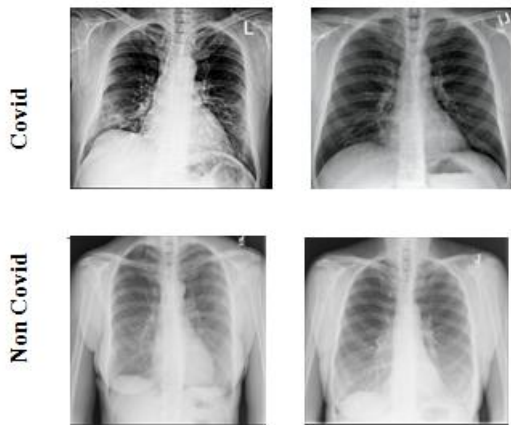


Figure 1: Samples of chest X-ray images from the dataset.

2.2 Image enhancement techniques

Image enhancement is a very important task used in image pre-processing. Its aim is to improve the visual details of an image or to provide a transform representation for an appropriate usage in different fields [4, 11]. In this paper, we have considered the following enhancement techniques.

2.2.1 Histogram equalization

Histogram Equalization (HE) is a technique for adjusting the contrast of an image using the image's histogram. The goal of Histogram Equalization is to obtain a uniform histogram, which improves contrast [13].

2.2.2 Contrast limited adaptive histogram equalization

Contrast Limited Adaptive Histogram Equalization (CLAHE) was originally developed for the enhancement of low-contrast medical images. The algorithm of CLAHE creates non-overlapping contextual regions (also called sub-images, tiles or blocks) and then applies the histogram equalization to each contextual region, clips the original histogram to a specific value and then redistributes the clipped pixels to each gray level. The clipping level determines how much noise in the histogram should be smoothed and hence how much the contrast should be enhanced [13].

2.2.3 Gamma correction

Gamma Correction (GC) is a nonlinear adaptation applied to each and every pixel value. Gamma corrections alternate the pixel value to improve the image using the projection relationship between the value of the pixel and the value of gamma according to the internal map. To calculate the gamma correction, the input value is raised to the power of the inverse gamma. The formula for this is as follows [13]:

$$\hat{i} = 255 \left(\frac{1}{255} \right)^{\frac{1}{\gamma}} \quad (1)$$

Values of $\gamma < 1$ will shift the image towards the darker end of the spectrum while $\gamma > 1$ will make the image appear lighter. $\gamma = 1$ will have no effect on the input image.

The application of histogram equalization (HE), Contrast Limited Adaptive Histogram Equalization (CLAHE), gamma correction, and their combination significantly improves the quality of COVID-19 X-ray images, aiding in better feature visualization and extraction (see Figure 2).

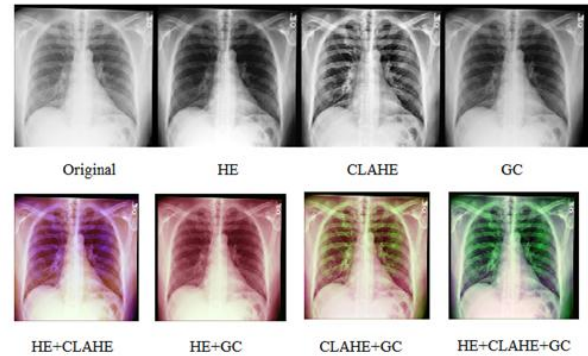


Figure 2: X-ray image processed with various image enhancement techniques.

Histogram equalization enhances global contrast, making subtle abnormalities more visible, while CLAHE adaptively improves local contrast, preserving fine details and reducing noise amplification. Gamma correction adjusts image brightness non-linearly, enhancing low-intensity features like ground-glass opacities. When combined, these techniques provide a comprehensive enhancement by leveraging global and local adjustments, ultimately producing images with improved visibility of critical diagnostic features. This preprocessing step enhances the performance of convolutional neural networks (CNNs) by supplying higher-quality inputs, resulting in superior COVID-19 detection accuracy and robustness.

2.3 Pre-trained CNN

Two different CNN models (ResNet50 [26] and DenseNet201 [27]) were compared separately using eight different image enhancement techniques for the classification of COVID-19 and non-COVID to investigate the effect of image enhancement on COVID-19 detection.

2.4 Performance metrics

In order to evaluate the performance of each deep learning model, different metrics have been applied in this study [13,28]:

$$Accuracy = \frac{TP+TN}{TP+TN+FP+FN} \quad (2)$$

$$Sensitivity = \frac{TP}{TP+FN} \quad (3)$$

$$Specificity = \frac{TN}{TN+FP} \quad (4)$$

$$F1 - Score = \frac{2TP}{2TP+FP+FN} \tag{5}$$

where:

True Positive (TP): The prediction is COVID and the image is COVID.

True Negative (TN): The prediction is non COVID and the image is non COVID.

False Positive (FP): The prediction is COVID and the image is non COVID.

False Negative (FN): The prediction is non COVID and the image is COVID.

2.5 Methodology

Firstly, we train and test two pre-trained convolutional neural networks with original CXR images, and then we repeat the same operation with the same images enhanced with the two techniques cited below. The major experiments that are carried out in this study are the combination of the enhancement methods; HE and CLAHE; CLAHE and GC; HE and GC and finally CLAHE, HE and GC (see Figure 2). For each combination, we compute the four performance metrics rates. The detailed methodology adopted in the study is shown in Figure 3.

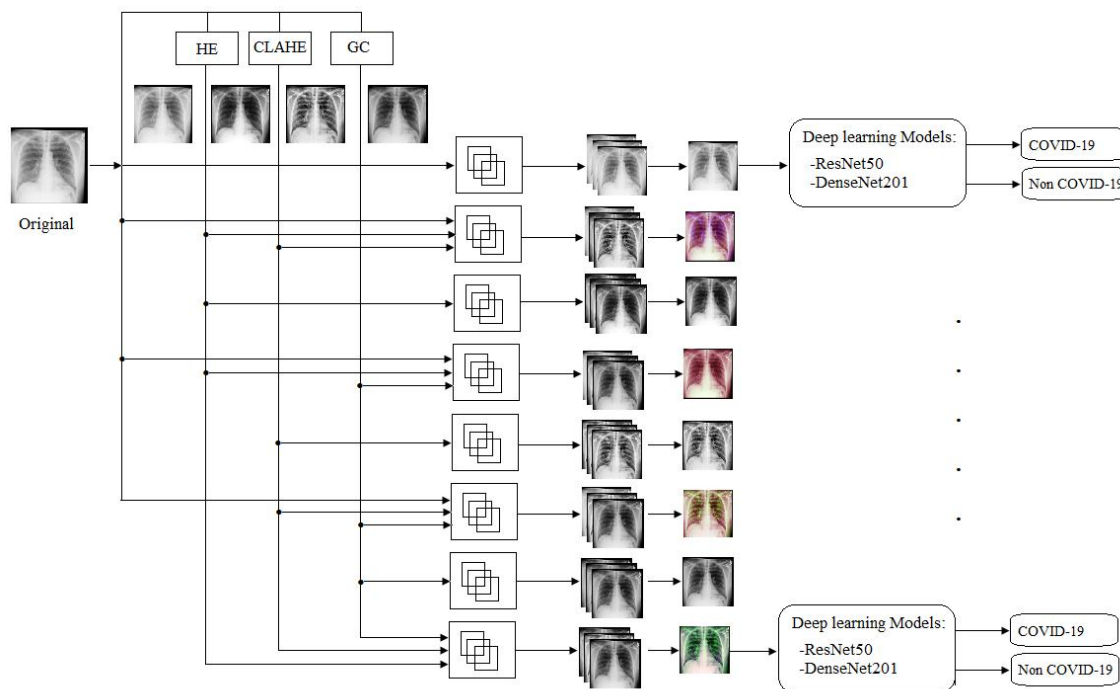


Figure 3: Flowchart of the proposed method.

3 Results

Firstly, the X-ray images were enhanced using the different techniques mentioned above. The concatenates are formed either from the original images (without enhancement), images enhanced by a single technique (HE, CLAHE, or GC), or by a combination of these. The obtained images allow us to build 8 databases. Secondly, we train two pre-trained networks; ResNet50, and DenseNet201 for detecting COVID-19 in chest X-ray scan images. The last fully connected layer of the pre-trained neural networks was modified to classify two classes: COVID-19 positive and negative. For both pre-trained networks, the learning rate was set to 0.0003, while the validation frequency was set to every 5 steps to track model performance. The maximum number of epochs was limited to 6, and the minimum batch size was set to 10. The Adam optimizer and the cross-entropy loss function were chosen. Additionally, data augmentation techniques were applied, including random rotations (-10,10) random horizontal and vertical shifting (-30,30)

and random scaling (0.5 1.1). Performance metrics were evaluated using 10 repeated cross-validation runs, each processing randomly selected image sets for training and testing.

3.1 Results without enhancement

In this part, we train and test the two networks using images without any enhancement. The DenseNet201 and the ResNet50 have achieved performance with an accuracy of 98.08% and 98.35% respectively. The confusion matrix constructed from the test evaluation results is shown in Figure 4.

3.2 Results with enhancement

The confusion matrix in Figure (5) illustrates the performance of DenseNet201 and ResNet50 models with different image enhancement techniques. In the case of DenseNet201 using CLAHE and GC techniques, a high accuracy of 99.68% was achieved with only 1 misclassification out of 312 samples.

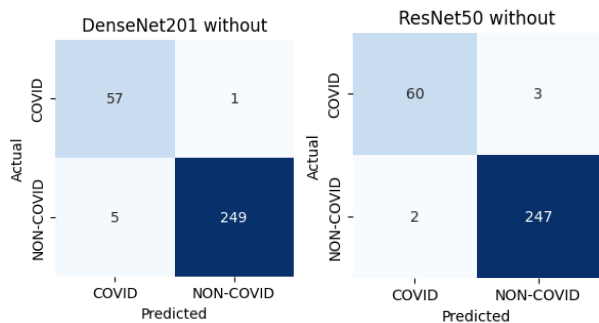


Figure 4: Confusion matrices for DenseNet 201 and RestNet 50 without enhancement.

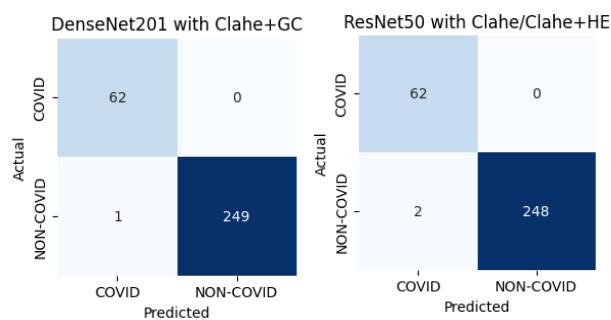


Figure 5: Confusion matrices for DenseNet 201 and RestNet 50 with enhancement.

The model demonstrates perfect recall (100%) for detecting COVID cases and a very high precision of 98.4%, indicating its ability to correctly identify COVID with minimal false negatives. Similarly, for NON-COVID cases, the recall and precision are near-perfect at 99.6% and 100%, respectively, showing excellent discrimination between the classes.

In the other hand, the ResNet50 model, utilizing HE, CLAHE, or a combination of CLAHE with HE or GC, demonstrates excellent performance with an accuracy of 99.36%. Out of 312 samples, the model correctly classifies 62 COVID cases and 248 NON-COVID cases, with only 2 misclassifications: 2 False Positives (NON-COVID predicted as COVID) and no False Negatives (COVID misclassified as NONCOVID). The recall for COVID detection is perfect at 100%, indicating no incorrect predictions of COVID for NON-COVID cases, while the precision is slightly lower at 96.9% due to the False Positives. These preprocessing techniques enhance image contrast and normalize brightness, aiding the model’s ability to discriminate between classes effectively.

4 Discussion

The performance metrics reported in Tables 2 and 3 provide a comprehensive comparison of different image enhancement techniques applied to ResNet50 and DenseNet201 models. The analysis includes accuracy, sensitivity, specificity, and F1-score, along with their respective standard deviations.

From Table 2, it is evident that histogram equalization (HE) and contrast-limited adaptive

histogram equalization (Clahe) generally improve the classification performance compared to the original images. The highest accuracy (98.17% ± 0.64) is achieved using the HE enhancement technique, with an F1-score of 98.86% ± 0.40. Clahe also performs well, achieving an accuracy of 98.07% ± 0.93 and the highest F1-score of 98.81% ± 0.57. This indicates that contrast enhancement techniques effectively highlight important features in the images, leading to improved model performance. However, the combination of enhancement techniques such as HE+GC and Clahe+GC does not consistently outperform individual techniques. For instance, HE+Clahe+GC results in a lower accuracy (97.43% ± 0.56) compared to HE alone, though it provides the highest specificity (93.38% ± 4.46). The standard deviation (SD) values suggest that these combined methods may introduce more variability in performance, as seen in specificity values.

Table 3 demonstrates that the DenseNet201 model generally exhibits higher accuracy compared to ResNet50 for most enhancement techniques. The best performance is achieved using the combined HE+Clahe+GC technique, yielding an accuracy of 99.03% ± 0.54 and an F1-score of 99.39% ± 0.34. This suggests that DenseNet201 is better at leveraging the enhanced features provided by multi-enhancement approaches. Among individual techniques, HE and Clahe both result in comparable accuracy (97.40% ± 0.82 and 97.30% ± 1.13, respectively), with Clahe producing a slightly higher F1-score of 98.32% ± 0.71. The GC technique results in relatively lower specificity (90.32% ± 2.94) compared to other methods, indicating that while it improves sensitivity, it may not be as effective in distinguishing negative cases.

Comparing the two models, DenseNet201 consistently outperforms ResNet50 across all enhancement techniques, with higher accuracy and F1-score values. The sensitivity of DenseNet201 is slightly lower in some cases but remains competitive. Specificity improvements are more pronounced in DenseNet201, which indicates better handling of false positives. Regarding variability, DenseNet201 exhibits lower standard deviations in most metrics, particularly in accuracy and F1-score, suggesting more stable and reliable performance across different enhancement techniques. Conversely, the ResNet50 model experiences greater variability, especially with specificity values. The results highlight the importance of image enhancement techniques in improving deep learning model performance. While individual techniques such as HE and Clahe provide significant improvements, combining multiple techniques can further enhance performance, particularly for DenseNet201.

In addition, while exploring the confidence intervals through error bars in Figure (6), It can be shown that the DenseNet201 model generally achieves higher accuracy and F1-scores, particularly with the combination of HE, Clahe and GC techniques, while ResNet50 shows better specificity for techniques like GC and HE+GC. Sensitivity remains high for both models, with

overlapping confidence intervals indicating comparable performance.

Table 2: Mean and Standard Deviation (SD) of Performance metrics for the ResNet50 model

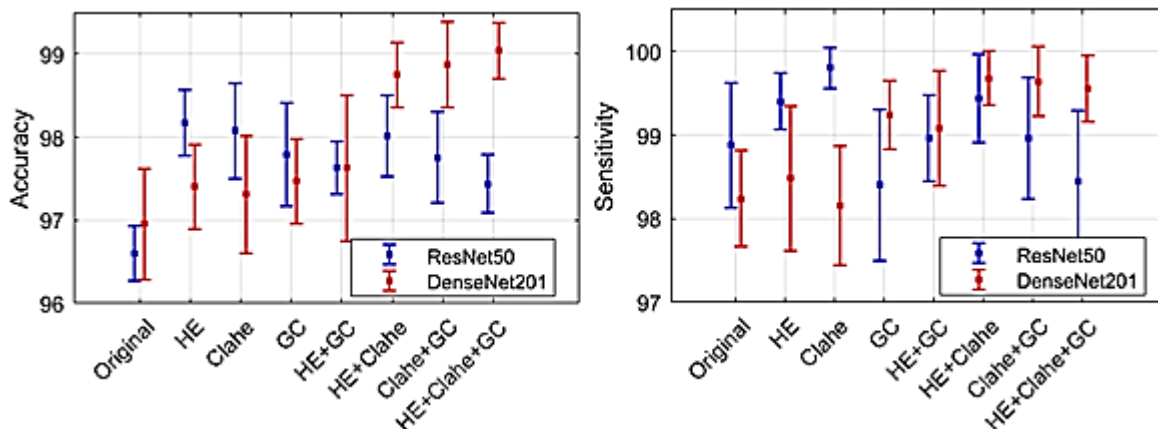
Enhancement Techniques	Accuracy (%)		Sensitivity (%)		Specificity (%)		F1-Score (%)	
	Mean	SD	Mean	SD	Mean	SD	Mean	SD
Original	96.60	0.52	98.88	1.20	87.41	5.67	97.90	0.31
HE	98.17	0.64	99.40	0.54	93.22	3.20	98.86	0.40
Clahe	98.07	0.93	99.80	0.38	91.12	4.04	98.81	0.57
GC	97.78	0.99	98.40	1.46	95.32	2.68	98.61	0.63
HE+GC	97.62	0.50	98.96	0.82	92.25	3.46	98.53	0.31
HE+ Clahe	98.01	0.78	99.44	0.84	92.25	2.49	98.77	0.49
Clahe+GC	97.75	0.89	98.96	1.16	92.90	3.58	98.60	0.56
HE+Clahe+GC	97.43	0.56	98.44	1.36	93.38	4.46	98.40	0.36

Table 3: Mean and Standard Deviation (SD) of Performance metrics for the DenseNet201 model

Enhancement Techniques	Accuracy (%)		Sensitivity (%)		Specificity (%)		F1-Score (%)	
	Mean	SD	Mean	SD	Mean	SD	Mean	SD
Original	96.95	1.08	98.24	0.92	91.77	4.95	98.10	0.66
HE	97.40	0.82	98.48	1.39	93.06	4.56	98.38	0.51
Clahe	97.30	1.13	98.16	1.15	93.87	4.15	98.32	0.71
GC	97.46	0.81	99.24	0.66	90.32	2.94	98.43	0.50
HE+GC	97.62	1.41	99.08	1.10	91.77	5.01	98.52	0.87
HE+ Clahe	98.75	0.63	99.68	0.52	95.00	2.89	99.22	0.38
Clahe+GC	98.87	0.83	99.64	0.66	95.80	2.17	99.30	0.51
HE+Clahe+GC	99.03	0.54	99.56	0.63	96.93	2.45	99.39	0.34

ResNet50 exhibits greater variability across metrics, whereas DenseNet201 provides more stable results. In addition, while exploring the confidence intervals through error bars in Figure (6), it can be shown that the DenseNet201 model generally outperforms ResNet50, particularly in Sensitivity and F1-score, with significant improvements observed when using combined enhancement techniques. However, DenseNet201

exhibits larger confidence intervals, indicating greater variability in its performance, whereas ResNet50 shows more consistent results with narrower confidence intervals, especially in Specificity. This variability suggests that while DenseNet201 may achieve higher performance, its predictions are less stable across trials or datasets.



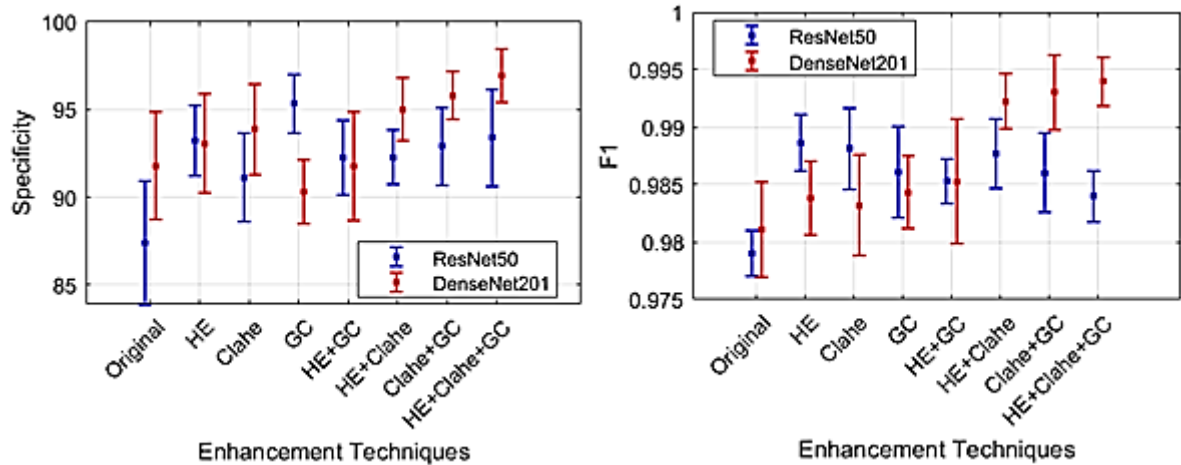


Figure 6: Confidence intervals for performance metrics of COVID-19 detection models.

The radar chart shown in Figure (7) compares the area under the ROC curve (AUC-ROC) for the two deep learning models across the different image preprocessing techniques. It can be seen that DenseNet201 generally demonstrates higher AUC-ROC values compared to ResNet50 across most preprocessing techniques, particularly in combinations involving multiple enhancements like HE+Clahe+GC and Clahe+GC. However, ResNet50 shows comparable performance in cases such as HE and GC. The results indicate that preprocessing techniques significantly impact model performance, with DenseNet201 being more responsive to enhancements. This suggests that model selection and preprocessing strategy should be carefully considered to optimize classification performance based on the desired evaluation metric.

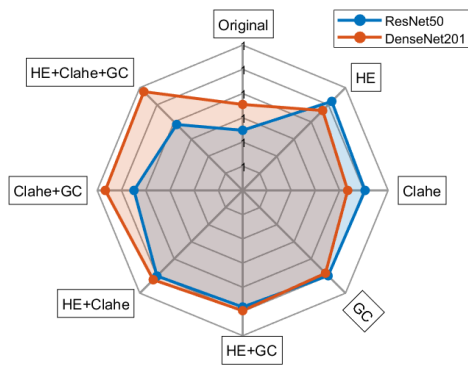


Figure 7: Radar plot of the area under the ROC curve (AUC-ROC) Performance for ResNet50 and DenseNet201 with Various Image Preprocessing Techniques.

5 Comparison with the state-of-the-art CNN approaches

To evaluate the proposed method, we made a comparison with some existing models using COVID-19 X-ray images. Narin et al. [7] have proposed three different DL

models. They achieved 96.1% accuracy on a dataset containing 3141 chest X-ray images. Ozturk et al. [5] have used the DarkCovidNet and the same dataset used in this paper. They achieved an accuracy of 98.08 %.

Purohit et al. [6] have used a Convolutional Neural Network with augmented data to increase the dataset. They have achieved 99.44 % accuracy.

In addition, the proposed enhancement methods show significant improvements in accuracy compared to the models using other data sets. The DenseNet201 model achieved an accuracy of 99.67%, outperforming models like Feki et al. [21], which reported 95.3% accuracy using Deep CNN, and Guefrechi et al. [20], which achieved 97.20% with a deep learning approach. Similarly, ResNet50 demonstrated high performance with an accuracy of 99.35%, surpassing Apostolopoulos et al. [17] (96.78%) and Mahmoud et al. [18] (97.40%). Furthermore, Deng et al. [15] achieved a maximum accuracy of 84.0%, showcasing the substantial improvement offered by the proposed methods. These results demonstrate that the proposed models consistently achieve higher accuracy, emphasizing their reliability and effectiveness in improving COVID-19 detection compared to the previously established state-of-the-art models.

6 Conclusion

This paper investigates how image enhancement techniques can improve the performance of pre-trained neural networks when working with limited data. Two pre-trained convolutional neural networks, ResNet50 and DenseNet201, were selected for COVID-19 detection. The training set was constructed by applying various enhancement techniques to chest X-ray images, which highlight critical structures such as lung opacities and consolidations—key features for accurate COVID-19 diagnosis. The results demonstrate that COVID-19 detection accuracy is significantly improved when using enhanced images compared to non-enhanced ones for both pre-trained networks.

Based on metrics such as accuracy, sensitivity, specificity, and F1-score, the best-performing model was DenseNet201, achieving an accuracy of 99.67%, sensitivity of 100%, specificity of 98.38%, and an F1-score of 99.80% for classifying positive and negative

cases. When compared to previous studies using the same dataset, DenseNet201 outperforms DarkCovidNet, which achieved 98.08%, underscoring the effectiveness of these enhanced models on real-world X-ray images.

Table 4: Results comparison with related works on COVID-19 detection

Sources	Method/Model	Samples	Accuracy (%)
[7]	Inception V3, ResNet50, Inception-ResNet V2	3141	96.1
[5]	DarkCovidNet	625	98.08
[6]	CNN	1072	99.44
[15]	SVM, CNN, ResNet50, Xception, VGG16	5857	84.00
[17]	VGG16, VGG19, ResNet, DenseNet, InceptionV3	1427	96.78
[18]	COVID-Net	610	97.40
[20]	Deep Learning	5000	97.20
[21]	Deep CNN	216	95.30
[29]	End-to-end CNN	5184	95.70
Proposed	ResNet50 with HE	625	99.36
	DenseNet201 with Clahe+HE+GC	625	99.67

References

- [1] Janko V, Slapničar G, Dovgan E, Reščič N, Kolenik T, Gjoreski M, Smerkol M, Gams M, Luštrek M. Machine Learning for Analyzing Non-Countermeasure Factors Affecting Early Spread of COVID-19. *International Journal of Environment Research and Public Health*, 18(13):6750, 2021. <https://doi.org/10.3390/ijerph18136750>
- [2] Rajkumar S, Rajaraman PV, Meganathan HS, Sathagirivasan V, ejaswinee V, Ashwin R. COVID-detect: a Deep Learning Approach for Classification of Covid-19 Pneumonia From Lung Segmented Chest Xrays. *Biomedical Engineering: Applications, Basis and Communications* 33(2), 2021. <https://doi.org/10.4015/S1016237221500101>
- [3] Gams M, Kolenik, T. Relations between Electronics, Artificial Intelligence and Information Society through Information Society Rules. *Electronics*, 10(4), 514, 2021. <https://doi.org/10.3390/electronics10040514>
- [4] Tahir A, Qiblawey Y, Khandakar A, Rahman T, Khurshid U, Musharavati F, Islam MT, Kiranyaz S, Al-Maadeed S, Chowdhury MEH. Deep Learning for Reliable Classification of COVID-19, MERS, and SARS from Chest X-ray Images. *Cognitive Computation*. 14:1752-1772, 2022. <https://doi.org/10.1007/s12559-021-09955-1>
- [5] Ozturk T, Talo M, Yildirim EA, Baloglu UB, Yildirim O, Acharya UR. Automated detection of covid-19 cases using deep neural networks with x-ray images, *Computers in Biology and Medicine*. 121(103792), 2020. <https://doi.org/10.1016/j.compbiomed.2020.103792>
- [6] Purohit K, Kesarwani A, Ranjan Kisku D, Dalui M. COVID-19 Detection on Chest X-Ray and CT Scan Images Using Multi-image Augmented Deep Learning Model. *Advances in Intelligent Systems and Computing*, 1412:395–413, 2022. http://dx.doi.org/10.1007/978-981-16-6890-6_30
- [7] Narin A, Kaya C, Pamuk Z. Automatic Detection of Coronavirus Disease (COVID-19) Using X-ray Images and Deep Convolutional Neural Networks, *Pattern Analysis and Applications* 24(3):1207–1220, 2020. <https://doi.org/10.1007/s10044-021-00984-y>
- [8] Sarki R, Ahmed K, Wang H, Zhang Y, Wang K. Automated detection of COVID-19 through convolutional neural network using chest x-ray images. *PLoS ONE* 17(1), 2022. <https://doi.org/10.1371/journal.pone.0262052>
- [9] Masud, M. A light-weight convolutional Neural Network Architecture for classification of COVID-19 chest X-Ray images. *Multimedia Systems*, 28:1165–1174, 2022. <https://doi.org/10.1007/s00530-021-00857-8>
- [10] Ravi, V, Narasimhan, H, Chakraborty, C et al. Deep learning-based metaclassifier approach for COVID-19 classification using CT scan and chest X-ray images. *Multimedia Systems*, 28:1401–1415, 2022. <https://doi.org/10.1007/s00530-021-00826-1>
- [11] Asif S, Zhao M, Tang F et al. A deep learning-based framework for detecting COVID-19 patients using chest X-rays. *Multimedia Systems*, 28:1495–1513, 2022. <https://doi.org/10.1007/s00530-022-00917-7>
- [12] Tahir A, Qiblawey Y, Khandakar A, Rahman T, Khurshid U, Musharavati F, Islam MT, Kiranyaz S, Al-Maadeed S, Chowdhury MEH. Exploring the effect of image enhancement techniques on COVID-19 detection using chest X-ray images. *Computers in Biology and Medicine*, 132, 2021. <https://doi.org/10.1016/j.compbiomed.2021.104319>

- [13] Kandhway P, Bhandari AK, Singh A. A novel reformed histogram equalization based medical image contrast enhancement using krill herd optimization, *Biomedical Signal Processing and Control*, 56 (101677), 2020.
<https://doi.org/10.1016/j.bspc.2019.101677>
- [14] Zhang J, Xie Y, Pang G, Liao Z, Verjans J, Li W, Sun Z, He J, Li Y, Shen C et al. Viral Pneumonia Screening on Chest X-Rays Using Confidence Aware Anomaly Detection. *IEEE Transaction on Medical Imaging*, 40(3): 879–890, 2021.
<https://doi.org/10.1109/tmi.2020.3040950>
- [15] Deng X, Shao H, Shi L, Wang X, Xie T. A classification–detection approach of COVID-19 based on chest X-ray and CT by using keras pretrained deep learning models. *Computer Modeling in Engineering & Sciences*. 125(2):579–596, 2020.
<https://doi.org/10.32604/cmescs.2020.011920>
- [16] Wang Z, Zhang K, Wang B. Detection of COVID-19 Cases Based on Deep Learning with X-ray Images. *Electronics*. 11(21):3511, 2022.
<https://doi.org/10.3390/electronics11213511>
- [17] Apostolopoulos, I.D, Mpesiana T.A. COVID-19: Automatic detection from X-ray images utilizing transfer learning with convolutional neural networks. *Physical and Engineering Sciences in Medicine*. 43: 635–640, 2020.
<https://doi.org/10.1007/s13246-020-00865-4>
- [18] Mahmud T, Rahman A, Fattah S.A. CovXNet: A multi-dilation convolutional neural network for automatic COVID-19 and other pneumonia detection from chest X-ray images with transferable multireceptive feature optimization. *Computers in Biology and Medicine*, 122, 103869,2020.
<https://doi.org/10.1016/j.compbiomed.2020.103869>
- [19] Mohit K, Dhairyata S, Vinod K, and Wanich S. COVID-19 prediction through X-ray images using transfer learning-based hybrid deep learning approach. *MaterialsToday: Proceeding*. 51: 2520–2524, 2022.
<https://doi.org/10.1016/j.matpr.2021.12.123>
- [20] Guefrechi S, Jabra M. B, Ammar A, Koubaa A, and Hamam H. Deep learning-based detection of COVID-19 from chest X-ray images. *Multimedia tools and applications*, 80: 31803-31820, 2021.
<https://doi.org/10.1007/s11042-021-11192-5>
- [21] Feki I, Ammar S, Kessentini Y, Muhammad K. Federated learning for COVID-19 screening from Chest X-ray images, *Applied Soft Computing*, 106, 2021.
<https://doi.org/10.1016/j.asoc.2021.107330>
- [22] Mohan A, Ftsum bAa, Beshir K, Takore TT. A Hybrid Deep Learning CNN model for COVID-19 detection from chest X-rays, *Heliyon*, 10(5), 2024.
<https://doi.org/10.1016/j.heliyon.2024.e26938>
- [23] Malik H, Naeem A, Naqvi, R A, and Loh, W. K. DMFL-Net: A Federated Learning-Based Framework for the Classification of COVID-19 from Multiple Chest Diseases Using Xrays. *Sensors*, 23(2):743, 2023.
<https://doi.org/10.3390/s23020743>
- [24] Gulmez, B. A novel deep neural network model based Xception and genetic algorithm for detection of COVID-19 from Xray images. *Annals of Operations Research*, 328:617–641, 2022.
<https://doi.org/10.1007/s10479-022-05151-y>
- [25] Zakariya A, Oraibi SA. Efficient COVID-19 Prediction by Merging Various Deep Learning Architectures, *Informatica* 48(5): 55–62, 2024.
<https://doi.org/10.31449/inf.v48i5.5424>
- [26] He K, Zhang X, Ren S, Sun J. Deep residual learning for image recognition, *Proceedings of the IEEE Conference on Computer Vision and Pattern Recognition*.2016.
<https://doi.org/10.1109/CVPR.2016.90>
- [27] Huang G, Liu Z, Van Der Maaten L, Weinberger KQ. Densely connected convolutional networks, *Proceedings of the IEEE Conference on Computer Vision and Pattern Recognition*. 2017.
<https://doi.ieeecomputersociety.org/10.1109/CVPR.2017.243>
- [28] Patel S, Patel L. Deep Learning Architectures and its Applications: A Survey, *International journal of computer sciences and engineering*. 6(6):1177-1183, 2018 .
<http://dx.doi.org/10.26438/ijcse/v6i6.11771183>
- [29] Zakariya A. Oraibi, Safaa Albasri. A Robust End-to-End CNN Architecture for Efficient COVID-19 Prediction from X-ray Images with Imbalanced Data, *Informatica*, 47(7):115–126, 2023.
<https://doi.org/10.31449/inf.v47i7.4790>

